Journal of Environmental Radioactivity 278 (2024) 107486

Contents lists available at ScienceDirect

Journal of Environmental Radioactivity

journal homepage: www.elsevier.com/locate/jenvrad

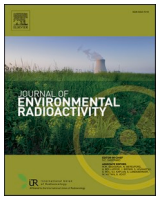

Chemical implication of the partition coefficient of ^{137}Cs between the suspended and dissolved phases in natural water

Katsumi Hirose [a,*], Yuichi Onda [b], Hirofumi Tsukada [c], Yuko Hiroyama [d], Yukiko Okada [e], Yoshikazu Kikawada [d]

[a] Laboratory for Environmental Research at Mount Fuji, Shujyuku-ku, Tokyo, 169-0072, Japan
[b] Center for Research in Isotopes and Environmental Dynamics, University of Tsukuba, Tsukuba, Ibaraki, 305-0006, Japan
[c] Institute of Environmental Radioactivity, Fukushima University, Fukushima-City, Fukushima, 960-1296, Japan
[d] Department of Materials and Life Sciences, Faculty of Science and Technology, Sophia University, Kioi-Cho, Chiyoda-ku, Tokyo, 102-8554, Japan
[e] Atomic Energy Laboratory, Tokyo City University, Ozenji 971, Asao-ku, Kawasaki, 215-0031, Japan

ARTICLE INFO

Handling Editor: Sheldon Landsberger

Keywords:
^{137}Cs
River water
Partition coefficient
Suspended sediment
Chemical model electric conductivity
Stable Cs

ABSTRACT

After the Fukushima Daiichi nuclear power plant accident, the terrestrial environment became severely contaminated with radiocesium. Consequently, the river and lake water in the Fukushima area exhibited high radiocesium levels, which declined subsequently. The partition coefficient of ^{137}Cs between the suspended sediment (SS) and dissolved phases, K_d, was introduced to better understand the dynamic behavior of ^{137}Cs in different systems. However, the K_d values in river water, ranging from 2×10^4 to 7×10^6 L kg^{-1}, showed large spatiotemporal variability. Therefore, the factors controlling the ^{137}Cs partition coefficient in natural water systems should be identified. Herein, we introduce a chemical model to explain the variability in ^{137}Cs K_d in natural water systems. The chemical model includes the complexation of Cs^+ with mineral and organic binding sites in SS, metal exchange reactions, and the presence of colloidal species. The application of the chemical model to natural water systems revealed that Cs^+ is strongly associated with binding sites in SS, and a major chemical interaction between ^{137}Cs and the binding sites in SS is the isotope exchange reaction between stable Cs and ^{137}Cs, rather than metal exchange reactions with other metal ions such as potassium ions. To explain the effect of the SS concentration on K_d, the presence of colloidal ^{137}Cs passing through a filter is significant as the dominant dissolved species of ^{137}Cs in river water. These results suggest that a better understanding of stable Cs dissolved in natural water is important for discerning the geochemical and ecological behaviors of ^{137}Cs in natural water.

1. Introduction

After the Fukushima Daiichi nuclear power plant (FDNPP) accident in 2011, a highly radioactively contaminated area was observed in the forested headwater catchment of the Tohoku and Kanto areas (Hirose, 2020; Onda et al., 2020; Povinec et al., 2013, 2021). Among the FDNPP-derived radionuclides, ^{137}Cs is the most important as it is a major radionuclide with a long radioactive half-life (30.2 y). Riverine systems are a major pathway for transporting FDNPP-derived ^{137}Cs from the forest to farmland, urban areas, and oceans. Therefore, an understanding of the migration of ^{137}Cs from radioactively contaminated catchments to rivers and the physical and chemical behaviors of ^{137}Cs in riverine systems is crucial. Radioactivity measurements of riverine systems have been conducted to assess the radiological effects of FDNPP-derived radiocesium in Fukushima Prefecture (Nagao et al., 2013, 2015; Onda et al., 2020 Sakaguchi et al., 2015). After the FDNPP accident, the Ministry of the Environment routinely measured ^{137}Cs in river water and riverbed sediments in eastern Japan.

The radiological monitoring of riverine systems has revealed spatiotemporal variations of ^{137}Cs in river water and riverbed sediments. Dissolved ^{137}Cs in stream water has shown a two-step decline over time (Iwagami et al., 2017a, 2017b; Taniguchi et al., 2019). A similar declining trend of ^{137}Cs in river water was observed after the Chernobyl accident (Nyléna and Grip, 1997; Smith et al., 2000, 2002). However, at short time scales, enhanced levels of dissolved ^{137}Cs have been recorded in river water under storm flow (Iwagami et al., 2019a, 2019b; Tsuji et al., 2016). To better understand the behavior of FDNPP-derived ^{137}Cs in river systems, the factors controlling ^{137}Cs

* Corresponding author.
E-mail address: hirose45037@mail2.acccsnet.ne.jp (K. Hirose).

https://doi.org/10.1016/j.jenvrad.2024.107486
Received 27 October 2023; Received in revised form 17 June 2024; Accepted 17 June 2024
Available online 26 June 2024
0265-931X/© 2024 Elsevier Ltd. All rights are reserved, including those for text and data mining, AI training, and similar technologies.

levels in river water should be elucidated.

Rivers are complex systems composed of inflowing rainwater and groundwater, including dissolved materials (inorganic ions, organics, and others) and suspended matter (soil particles, organisms and/or litters), where the direct injection of soil particles especially occurs during flood events (Tsuji et al., 2016); important processes are chemical interactions between target metals (toxic metals and radionuclides) and suspended sediment (SS) (and/or bottom sediment), and outflow of dissolved and suspended materials. SS plays an important role in the transport of ^{137}Cs, as 84%–92% of radiocesium is transported in SS form through the Abukuma River system, which is the largest river contaminated by the FDNPP-derived radionuclides (Yamashiki et al., 2014). The annual contribution of the ^{137}Cs discharge by SS was evaluated to be 96%–99% in the small headwater catchments of Yamakiya, located at the headwaters of the Abukuma River (Iwagami et al., 2017b).

Chemical interactions in the form of adsorption and desorption with soil minerals are important processes because ^{137}Cs is tightly associated with the binding sites of the soil (particularly, the clay component) (Beneš et al., 1989, 1992). The partition coefficient (or distribution coefficient; K_d) of ^{137}Cs between the dissolved and SS phases was introduced to better understand the migration from dissolved ^{137}Cs to suspended and/or sediment ^{137}Cs. The partition coefficient is a basic parameter for predicting radionuclide behavior in aquatic ecosystems (Boyer et al., 2018; IAEA, 1994, 2010). The applicability of K_d for modeling dissolved ^{137}Cs concentrations in the Fukushima River water has been examined; the results revealed that the model including K_d could not reproduce the seasonal variations of the dissolved ^{137}Cs concentrations in river water and under storm flow conditions, though it could reproduce the dissolved ^{137}Cs concentrations during the base flow period (Sakuma et al., 2018).

The partition coefficient of ^{137}Cs between the dissolved and SS phases, K_d, was determined for the rivers contaminated with FDNPP-derived ^{137}Cs. The results revealed large variability in the K_d values, ranging from 10^4 to 10^8 (Eyrolle-Boyer et al., 2016; Nagao et al., 2013; Osawa et al., 2018; Tsukada et al., 2017; Ueda et al., 2013; Yoshimura et al., 2015). The mean K_d values measured primarily in the Fukushima Prefecture after the FDNPP accident were a factor of 2–5 higher than those of previous observations in Japan after the Chernobyl fallout (Hirose et al., 1990) and global fallout (Matsunaga et al., 1991). To determine the factors controlling the partition coefficients of ^{137}Cs in river water, the correlations between K_d and water quality parameters, such as the SS concentrations and electric conductivity (EC), were examined, with the log-log plot of EC vs. K_d showing a negative correlation (Tsuji et al., 2019). However, the independence of K_d on SS concentration was not generally confirmed for the sorption of radiocesium on freshwater solids, as K_d has been found to increase (Madruga et al., 1988), decrease (Boyer et al., 2018; Mansfeld, 1980), and remain constant (Beneš et al., 1992; Yousef et al., 1970) with increasing concentrations of freshwater sediments.

Although soil particles are strongly bound to ^{137}Cs, a significant portion of the ^{137}Cs in the soil adsorbed on the frayed edge sites (FES) of clay minerals (Sawhney, 1972) is exchangeable with cations such as K^+ and NH_4^+ (Comans et al., 1989; Funaki et al., 2022; Hirose et al., 2015; Wauters et al., 1994). Notably, FES are extremely selective for Cs^+, K^+, NH_4^+, and Rb^+, weakly hydrated cations. The selectivity of FES for Cs^+, the highest among these monovalent ions, is approximately three orders of magnitude greater than that for K^+ and two orders of magnitude greater than that for NH_4^+ (Brouwer et al., 1983; McKinley et al., 2004; Nakao et al., 2008; Wauters et al., 1996). In other words, competitive reactions likely occurred between ^{137}Cs and K^+ (and other cations) in river water. Meanwhile, ^{137}Cs interacts with coarse organic substances (leaves and branches) (Iwagami et al., 2017b, 2019b), though the chemical mechanism of the interaction between ^{137}Cs and organic matter is unknown. Dissolved organic carbon concentrations correlated with dissolved radiocesium in headwater streams (Kawano et al., 2023), which showed seasonal change. Nevertheless, there is little information on the chemical reactions of ^{137}Cs with dissolved ligands, suspended particles, and bottom sediments in river water owing to the lack of knowledge of the chemical properties of the binding sites (ligands) in the dissolved, suspended, and sediment phases.

Trace elements in natural water, including radionuclides such as ^{137}Cs, are conventionally separated into dissolved and suspended particles by filtration with a pore size of 0.45 μm (Gustafsson and Gschwend, 1997). Therefore, dissolved elements are generally not pure solutes; colloids, operationally defined as phases within a range of 1000 Da ultrafilter and 0.45 μm filter cut-offs, are involved in the dissolved phase. In the 1980s, surface complexation models were developed to understand the basic interactions that occur at the oxide–solution interface, where Fe oxides are the major adsorbents (Honeyman and Santschi, 1988). The particle concentration effect, in which log K_d is negatively correlated with the logarithm of the particulate matter concentrations (log Cp), arises from the relative effect of the adsorbates associated with colloids but still operationally considered to be in the "dissolved" fraction (Higgo and Rees, 1986; Morel and Gschwend, 1987). A study using cascade filtrations (at 1.2, 0.4, and 0.025 μm) revealed the presence of colloidal carriers (dissolved organic material and inorganic nanoparticles in stream waters), in which many major elements (Na, Mg, Si, K, and Ca) showed no colloidal influence whereas the majority of trace metals (Al, Ti, V, Mn, Fe, Cu, Y, REE, and U) showed some influence in the chemistry of colloids (Trostle et al., 2016). Cesium is predominantly present in freshwater as a free cationic species, Cs^+ (Duursma and Eisma, 1973). A speciation study using sequential ultrafiltration revealed that ^{137}Cs in the Rhone River water was not significantly associated with the colloidal fraction (0.002–0.45 μm) under low water flow (Eyrolle and Charmasson, 2001). However, mineralogical studies have suggested that palygorskite and pyrophllite are present in colloidal fractions (Lagaly, 2006; Okumura et al., 2018). Colloidal clay minerals may significantly affect the chemical form of Cs in river water. However, little information is available on the geochemical and ecological roles of colloidal ^{137}Cs in Japanese river systems.

In this study, we describe the factors controlling the partitioning of ^{137}Cs in natural water systems using a chemical model of Cs based on radioactivity data from river water and irrigation waters observed on East Honshu Island, Japan, along with ^{137}Cs K_d values for coastal sediments from the pre-FDNPP-accident era (Kusakabe and Takata, 2020).

2. Measurements

Radioactivity data from river waters documented by the Ministry of the Environment (MOE, 2018) were used in this study. To analyze such data, which include stable cesium (^{133}Cs) concentrations in fresh water, we also used data from the irrigation water of Fukushima Prefecture, whose samples were collected during June–October 2014 (Tsukada et al., 2017). The river water samples and radiochemical measurements are briefly described as follows.

River water samples were collected from a bridge or riverbank (depth of 50 cm) by the Ministry of the Environment using a bucket or ladle in August 2017. The sampling sites were located in East Honshu Island (Iwate, Miyagi, Fukushima, Tochigi, Gunma, Ibaraki, and Chiba Prefectures). The sample volume was 3 L. Immediately after the sampling, the river water was filtered through a 0.45 μm pore size membrane filter. The filtrate is defined as the dissolved fraction. ^{137}Cs in the dissolved fraction was concentrated as an AMP (ammonium moybdophosphate) precipitate.

Samples of SS were collected using an SS sampler. Samplers were set up at each sampling point along the river. The samples, including the suspension, were kept still for 2–3 d, and the supernatant was removed. The residue was dried at 105 °C for 24 h for analysis. The particle size distribution of the suspended sediment (SS) in the river water sample was separately analyzed by laser diffraction (SALD3100, Shimadzu Co., Ltd, Tokyo, Japan) (Tsuji et al., 2019).

^{137}Cs in dissolved and SS fractions was measured using a high-purity

germanium gamma-ray well detector (GCW2022S, Canberra−Eurisys, Meriden), equipped with an amplifier (PSC822, Canberra, Meriden) and multichannel analyzer (DSA1000, Canberra, Meriden). The gamma-ray emission was measured at 662 keV. The analytical accuracy was certified by the World Wide Proficiency Test using standard soil samples from the International Atomic Energy Agency. Measurement was continued until the counting error in the measurement of ^{137}Cs activity was less than 10%, which required a measurement period of 1–24 h depending on the sample weight (Yoshimura et al., 2015).

All radionuclide data are available on the Environmental Radioactivity Datasets website at CRiES, University of Tsukuba (http://www.ied.tsukuba.ac.jp/database/0022.html).

3. Results and discussion

3.1. Dissolved and suspended ^{137}Cs in river waters

The concentrations of dissolved and suspended ^{137}Cs in river water in Fukushima Prefecture were recorded together with the concentrations of SS and EC (Supplementary Table 1S). The results of river waters, together with the irrigation water, are summarized in Table 1. The activity concentrations of dissolved and suspended ^{137}Cs in river water in August 2017 ranged from 0.1 to 122 mBq L^{-1} and 0.1–194 mBq L^{-1}, respectively. Both dissolved and suspended ^{137}Cs activity concentrations in river water exhibit a large spatial variability of greater than three orders of magnitude, which reflects the spatial distribution of the ^{137}Cs deposition density in the catchment area (Ochiai et al., 2015; Tsuji et al., 2014; Yoshimura et al., 2015).

Table 1
Outline of dissolved and suspended^{137}Cs activity concentrations in river water and irrigation water in Fukushima.

River water	Sample number: 40				
	Minimum	Maximum	Mean	Median	SD
SS ^{137}Cs Bq g^{-1}	0.16	23	2.5	1.2	3.8
Dissolved ^{137}Cs Bq L^{-1}	0.0001 ± 0.0001	0.122 ± 0.086	0.0084	0.0094	0.0081
SS mg L^{-1}	0.00078	0.0574	0.013	0.067	0.015
EC mS cm^{-1}	0.046	0.95	0.17	0.13	0.15
K_d L kg^{-1}	22000	7300000	880000	410000	1700000
Irrigation water[a]	Sample number: 54				
SS ^{137}Cs Bq g^{-1}	1.5 ± 0.1	300 ± 1.4	47	27	59
Dissolved ^{137}Cs Bq L^{-1}	0.007 ± 0.001	6.7 ± 0.086	0.19	0.66	0.24
SS mg L^{-1}	0.00078	0.0574	0.013	0.067	0.015
EC mS cm^{-1}	0.037	0.36	0.114	0.09	0.075
K mmol L^{-1}	0.0057	0.265	0.038	0.028	0.0427
Cs nmol L^{-1}	0.031	0.299	0.089	0.064	0.082
K_d L kg^{-1}	4100	2100000	110000	94000	370000

[a] Data referred from Tsukada et al. (2017).

To elucidate the geochemical behavior of ^{137}Cs in the river system, the partition coefficients of ^{137}Cs between the dissolved and suspended phases were calculated (Supplementary Table 1S). The partition coefficients ranged from 2.2 × 10^4 to 7.03 × 10^6 L kg^{-1}, representing the same order of magnitude as that documented for the FDNPP-derived ^{137}Cs (Nagao et al., 2013; Osawa et al., 2018; Tsukada et al., 2017; Ueda et al., 2013; Yoshimura et al., 2015). Notably, the partition coefficients of ^{137}Cs in the rivers of East Honshu Island showed large spatial variability.

3.2. Effect of coexistence of metal ions

In the MOE data, there is limited information on the relationship between the concentrations of the major components of the river waters and ^{137}Cs in monitoring sites. However, EC is commonly measured to assess the water quality in the river water samples. The EC in Japanese river waters is linearly correlated with the potassium concentration (MOE, 2018; Tsuji et al., 2019). If the EC is linearly related to the concentrations of competing metal ions, the partition coefficients are expected to be inversely related to the EC values, owing to the metal exchange reactions with competing metal ions (Appendix Eq. (16)). We examined the relationship between the EC values and partition coefficients of ^{137}Cs for SS in river waters, with the results shown in Fig. 1. Both partition coefficients are negatively correlated to the log EC values (correlation slope: −1.08 ± 0.21, intercept: 4.69 ± 0.19, correlation factor: 0.54). The slope of the log-log plots was near unity, as deduced from the chemical equilibrium model (Appendix Eq. (16)). This result suggests that dissolved ^{137}Cs exists in an ionic form, which is chemically likely because Cs is an alkali metal, and may imply that the lower K_d of ^{137}Cs in river water is due to metal exchange reactions with competing metal ions such as K^+. Tsukada et al. (2017) reported negative correlation between the log EC and log K_d in the irrigation waters. However, there was a large scatter in the log-log plots between the K_d and EC values. To recognize whether this correlation in the irrigation waters is real or not, we examined relationships between log EC values and log C_K (dissolved potassium concentration), and log C_{Cs} (dissolved stable cesium (^{133}Cs) concentration) (All data in the irrigation water are shown in Supplementary Table 2S). We found a good correlation between log EC and log C_K (slope: 1.04 ± 0.4, correlation factor: 0.699), while there was no correlation between log EC and log C_{Cs} (slope: 0.081 ± 0.21, correlation factor: 0.054) (Supplementary Fig. 1S). To confirm the correlation between log EC and log K_d in the irrigation waters, additional examination for a lower EC level (0.037–0.1 mS cm^{-1}) was carried out. The result is shown in Supplementary Fig. 2S. A poor positive correlation occurred between log K_d and log EC (slope: 0.85 ± 0.96, correlation

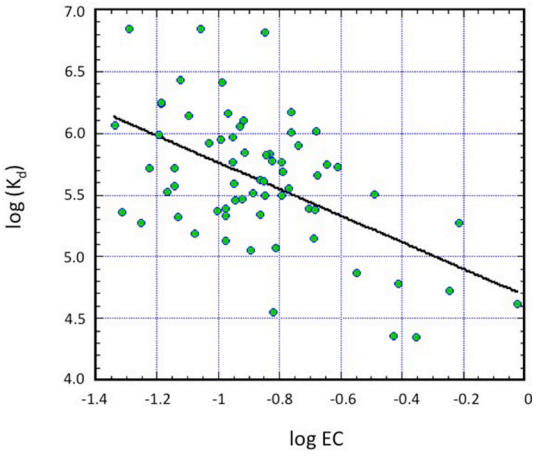

Fig. 1. Relationship between the partition coefficient, K_d, and the electric conductivity (EC) in the river waters of Fukushima Prefecture, Japan. Unit: kg L^{-1} (K_d), mS cm^{-1} (EC).

factor: 0.165), which was inconsistent with the previous results of negative correlation between log ES and log K_d (Tsuji et al., 2019; Tsukada et al., 2017). This finding suggests that the EC value in irrigation waters is not indicator related to the K_d values.

To gain a better understanding of the chemical processes in river water systems, it is important to obtain information on the chemical composition (especially ^{133}Cs and K) dissolved in river water. Tsukada et al. (2017) have reported ^{133}Cs and K concentrations dissolved in the irrigation (ponds and rivers) waters in Fukushima Prefecture (Supplementary Table 2S), as did the K_d of ^{137}Cs. We examined the relationship between ^{133}Cs and K concentrations in the irrigation waters in Fukushima Prefecture, finding no correlation, as shown in Fig. 2A, which is consistent with no correlation between EC and ^{133}Cs concentration (Supplementary Fig. 1S). As sea salts are a potential source of ^{133}Cs in freshwater, the ^{133}Cs/K ratio (0.216×10^{-6}; Chester, 2003) is shown in Fig. 2A. To examine how ^{133}Cs is compared with sea salt, enrichment factors based on K in sea salt ($EF_{Cs,\ sea}$) are introduced: $EF_{Cs,\ sea} = (C_{Cs,obs}/C_{K,obs})/C_{Cs,sea}/C_{K,sea})$, where $C_{Cs,obs}$ and $C_{K,obs}$ are the dissolved ^{133}Cs and K concentrations in the irrigation waters, respectively, and $C_{Cs,sea}$ and $C_{K,sea}$ are the dissolved ^{133}Cs and K concentrations in seawater, respectively. The results (Fig. 2B) revealed that the $EF_{Cs,\ sea}$ were greater than unity, except at one point, indicating that the ^{133}Cs concentrations in the irrigation waters were higher than those expected from the sea salt source, especially at lower K concentrations (<0.1 mM). Notably, the majority of the dissolved ^{133}Cs within 20 km of the FDNPP was enriched compared with that of sea salt, for which the maximum $EF_{Cs,sea}$ reached 120. This finding suggests that sources of dissolved ^{133}Cs other than sea salt exist within 20 km of the FDNPP. To elucidate the chemical effect of the K concentration on the K_d value of ^{137}Cs, log-log plots of K_d and K concentration in the irrigation waters were obtained, as shown in Fig. 3. There was no correlation between K_d and K concentration in the irrigation waters. Furthermore, log-log plot of K_d and K concentration for lower EC level (0.037–0.1 mS cm^{-1}) was carried out: a poor correlation (slope: 0.45 ± 0.37, correlation factor: 0.22) (Supplementary Fig. 3S). These findings suggest that the metal exchange reaction between ^{137}Cs and K is not a controlling process in determining K_d in the irrigation waters.

To elucidate the geochemical role of dissolved ^{133}Cs in the K_d values determined from ^{137}Cs in the irrigation waters, Tsukada et al. (2017) examined the relationship between K_d and ^{133}Cs concentration in the irrigation waters. The results revealed that the log K_d values correlated with the log ^{133}Cs concentration, residing in a band with a slope of unity (Fig. 4A). We examined log-log plots of K_d and ^{133}Cs concentration for the lower EC level (0.037–0.1 mS cm^{-1}) (Supplementary Fig. 4S). A good negative correlation appeared between K_d and ^{133}Cs concentration in the irrigation waters (slope: −0.94 ± 0.22, correlation factor: 0.63). The relationship between K_d and the dissolved ^{133}Cs suggests that the ^{133}Cs concentration dissolved in the irrigation waters primarily governs the K_d values, irrespective of the variability of the chemical compositions of the major components dissolved in the irrigation waters.

Radiocesium deposited on land is transported to the oceans via riverine processes. As the environment changes from river water to seawater, the chemical constituents, such as dissolved ion concentrations, of the medium change drastically. This process affects the behavior of radiocesium in the SS; typically, metal exchange reactions occur between ^{137}Cs in the SS and dissolved cationic ions such as Na^+ and K^+ (Takata et al., 2020, 2021). Leaching experiments using artificial seawater have revealed that several percent of the ^{137}Cs in SS is released into the dissolved phase (Yamasaki et al., 2016). However, there is no information on the behavior of ^{133}Cs during this leaching process. In contrast, leaching experiments using soil revealed that extractants with high ammonium ion concentrations can extract ^{133}Cs from soils, as does ^{137}Cs, in which the extracted portions of ^{137}Cs were higher than that of ^{133}Cs (Kikawada et al., 2015). Therefore, it is valuable to know whether the K_d values of ^{137}Cs for coastal bottom sediments exist in a band with a slope of unity, as observed in freshwater. Plots of the K_d values in coastal sediments to the ^{133}Cs concentrations (Fig. 4A) indicate that the plots were located on the extension of the band observed in river water. The

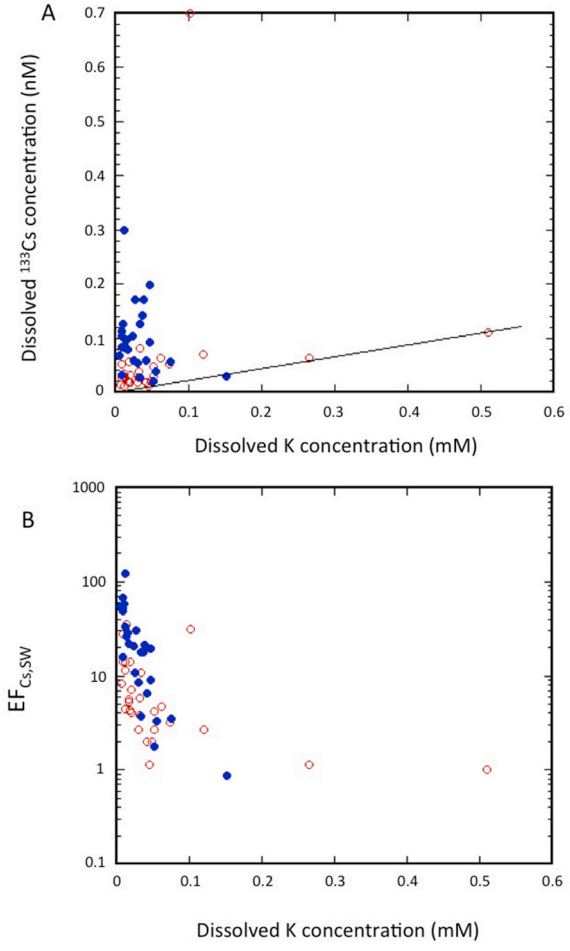

Fig. 2. A. Relationship between stable Cs and K concentrations in the irrigation water of Fukushima Prefecture. The solid line shows the Cs/K mole ratio of sea salt (Chester, 2003). B. Relationship between the enrichment factor (EF) of stable Cs and K concentrations in the irrigation waters. Blue closed circles: <20 km from the FDNPP, red open circles: 20 km–80 km from the FDNPP. (For interpretation of the references to colour in this figure legend, the reader is referred to the Web version of this article.)

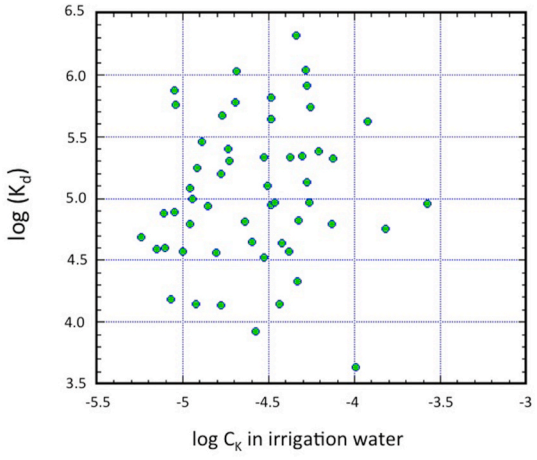

Fig. 3. Relationship between the partition coefficient and K concentration in the irrigation water. Unit: kg L^{-1} (K_d), mol L^{-1} (C_K).

finding suggests that the chemical mechanism characterizing the ^{137}Cs–SS interaction in irrigation waters is applicable to the interaction between ^{137}Cs and the coastal sediment. The ^{133}Cs level in Japanese river water was lower than that in seawater. However, the high ^{133}Cs concentration was observed in Yugama Crater lake, Kusatsu-Shirane volcano (15 nmol L^{-1}) (Hirayama et al., 2020). A lower K_d value may occur under the conditions of high ^{133}Cs. Experiment of ^{133}Cs addition to a^{137}Cs contaminated reservoir revealed that a significant amount of ^{137}Cs was released into lake water from sediment (Pinder III et al., 2005).

To better understand the chemical process between K_d and stable Cs in the river system, we examined the chemical model calculations of the three cases to reveal the relationship between the partition coefficients and stable Cs concentrations in river water. The chemical model (Appendix) revealed that the conditional stability constants and binding site concentrations are important parameters for calculating the K_d values. We assumed that two binding sites exist in SS; one possibility is that there is only one strong binding site (may be the FES of the clay mineral) reacting with Cs ($K'_{Cs,ss,1} = 10^{12}$), another possibility is only one weak binding site ($K'_{Cs,ss,2} = 10^{10}$), and finally the third possibility is the coexistence of weak and strong binding sites (Appendix Eq. (20)). The binding concentrations in the SS can be estimated under the conditions of chemical equilibrium: $C_{SS,ex133Cs}/C_{d,133Cs}$=$C_{SS,137Cs}/C_{d,137Cs}$ and $C_{L,ss,L} = C_{SS,ex133Cs} = K_{d,137Cs}$' $C_{d,133Cs}$. The binding site concentrations in the SS were estimated to be 0.49–52 μmol kg^{-1} with 9.4 μmol kg^{-1} as the average value. As tentative lower and upper limits of the binding-site concentration in the SS, $C_{L,ss,i}$, 10^{-6} and $10^{-4.5}$ mol kg^{-1} were used, respectively. The results for the one strong binding site case are shown in Fig. 4B, where the lower and upper limits are indicated by yellow and red dots, respectively. The single strong binding site model can cover a band that includes most of the observed values, considering variable binding-site concentrations. The single weak binding site model case with the same $C_{L,ss,L}$ and $C_{L,ss,U}$ values as the strong binding site model, yielded two curves, one representing a constant value below 10 pmol L^{-1} of ^{133}Cs and one characterized by a line above 1 nmol L^{-1} with slope −1 (Fig. 4B). The zone between the two curves for the second case cannot cover all observed values. These findings imply that the lower limit of the conditional stability constant of the Cs complex with the strong binding site, $K'_{Cs,ss,1}$, can be estimated to be $> 10^{11}$ M^{-1} based on the following relationship: $K_{Cs,ss,1}$ $[Cs^+] > 1$. In the third case,

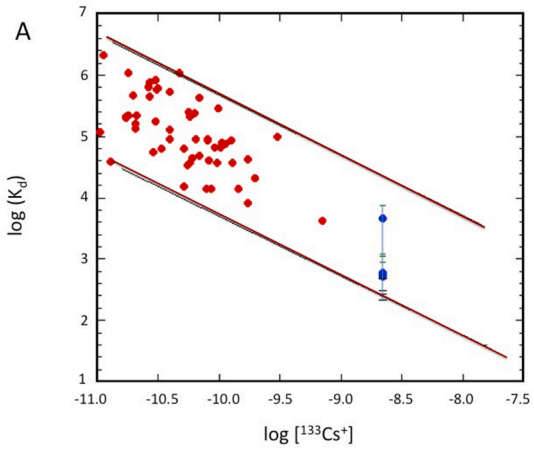

Fig. 4A. Relationship between the partition coefficient and stable Cs concentration in natural water. The solid curve shows a straight line with a slope of −1. Unit: kg L^{-1} (K_d), mol L^{-1} (C_{Cs}). Red dots: irrigation sediments, blue dots: mean values of K_d for marine coastal sediments off east Honshu Island (Aomori, Miyagi, Fukushima, Ibaragi), cited from Kusakabe and Takata (2020). The concentration of stable Cs in seawater is 2.2 nmol kg^{-1} (Chester, 2003). (For interpretation of the references to colour in this figure legend, the reader is referred to the Web version of this article.)

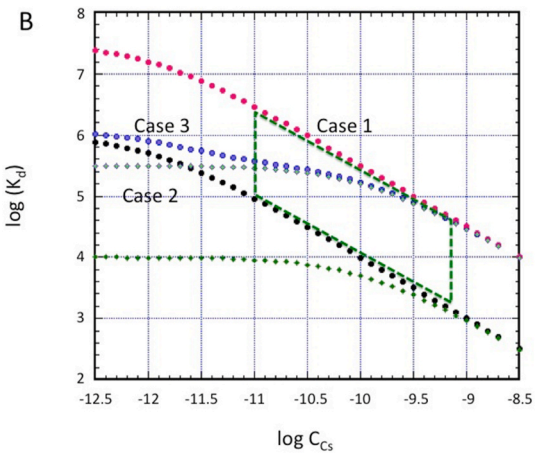

Fig. 4B. Relationship between the partition coefficient and Cs $^+$ concentration from the chemical model calculation. Case 1: strong binding site, red dot (f = $10^{-4.5}$), yellow dot (f = 10^{-6}); Case 2: weak binding site, pale green diamond (f = $10^{-4.5}$), green diamond (f = 10^{-6}); Case 3: two types of binding sites, blue dot (strong binding site (f = 10^{-6}) and weak binding site (f = $10^{-4.5}$). Area surrounded by the green dotted line represents one spread observation values. (For interpretation of the references to colour in this figure legend, the reader is referred to the Web version of this article.)

representing the coexistence of two binding sites, the model produced a more complicated curve between log K_d and log $[Cs^+]$, as indicated by the blue dot in Fig. 4B. Because the data were a composite obtained from different locations and sampling times, it was difficult to determine whether the two-binding-site model was adequate.

Tsukada et al. (2017) reported that the K_d values in the irrigation waters observed within 20 km of the FDNPP were significantly lower than those in the range from 20 km to 80 km (Fig. 5A), in which the log K_d values were calculated to be 3.92–5.81 with an average of 4.79 for sampling sites within 20 km of the FDNPP and 3.63–6.32 with an average of 5.37 for sampling sites from 20 km to 80 km of the FDNPP, respectively. The chemical model revealed that the ^{133}Cs concentrations dissolved in water were the key factors controlling the K_d values. The natural source of ^{133}Cs in fresh waters is assumed to be sea salt. The dissolved ^{133}Cs concentrations derived from natural sources ($C_{133Cs,n}$) were estimated from the potassium concentrations as follows:

$$C_{133Cs,n} = C_{K,obs}\ (C_{Cs,sea}/C_{K,sea}) \quad (1)$$

The ^{137}Cs concentration normalized by sea salt is calculated as follows:

$$C_{d137Cs,n} = (C_{d137Cs,obs}/C_{133Cs,\ obs})\ C_{133Cs,n} \quad (2)$$

We introduce the partition coefficient of ^{137}Cs normalized by sea salt, which is presented as follows:

$$K_{d,n} = C_{137Cs,ss}/\ C_{d137Cs,n} \quad (3)$$

The log $K_{d,n}$ values were calculated to be 4.71–7.10 with an average of 5.98 for sampling sites within 20 km of the FDNPP and 5.03–7.05 with an average of 6.07 for sampling sites from 20 km to 80 km of the FDNPP, respectively. As shown in Fig. 5B, the frequency distribution of $K_{d,n}$ within 20 km of the FDNPP coincides with that from 20 to 80 km of the FDNPP, implying that the $K_{d,n}$ values are independent of the distance from the FDNPP. This finding suggests that the occurrence of lower K_d values near the FDNPP is due to an increase in the ^{133}Cs dissolved in the irrigation waters and isotope exchange reactions. ^{133}Cs, which is also one of the fission products, is produced in a nuclear reactor. Hot particles (CsMPs: ^{137}Cs-enriched particles) emitted from the FDNPP accident contained ^{133}Cs at the same order of magnitude as the mass amount of ^{137}Cs (Adachi et al., 2013; Igarashi et al., 2019). However, it is difficult

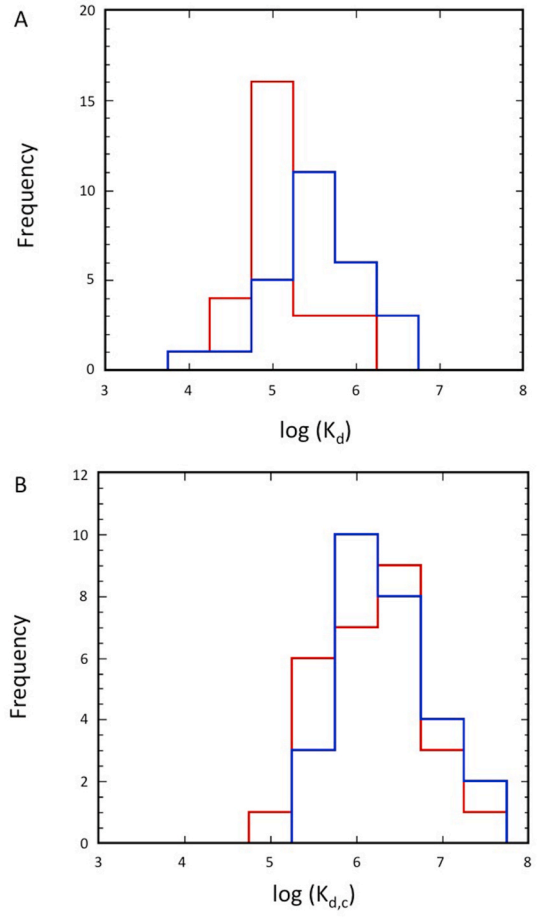

Fig. 5. A. Frequency distributions of log K_d in the irrigation water. B. Frequency distributions of log normalized K_d. Blue line: <20 km from the FDNPP, red line: 20 km–80 km from the FDNPP. (For interpretation of the references to colour in this figure legend, the reader is referred to the Web version of this article.)

to explain the high levels of dissolved ^{133}Cs near the FDNPP as being caused by the emission of ^{133}Cs by the FDNPP accident, because the concentrations of excess dissolved ^{133}Cs observed in the irrigation waters were much higher than the mass concentration of ^{137}Cs.

The conditional stability constant of the Cs complex estimated from the chemical model is much greater than the previous one for illite ($10^{6.95}$; 0.1 M Na^+) (Poinssot et al., 1999), which is consistent with the lower K_d values (log K_d = 4.7) determined by leaching experiments. However, the K_d values for FDNPP-derived radiocesium were higher than 10^5 (Eyrolle-Boyer et al., 2016; Miura et al., 2018; Nagao et al., 2013; Osawa et al., 2018; Tsukada et al., 2017; Ueda et al., 2013; Yoshimura et al., 2015), which is one or two orders of magnitude higher than that of Chernobyl (Konoplev et al., 2016). The high conditional stability constant of the Cs complex in freshwater after the FDNPP accident may be explained by two hypotheses: the contribution of insoluble ^{137}Cs-enriched particles (CsPMs) (Igarashi et al., 2019; Konoplev et al., 2016; Miura et al., 2018) or the effect of low cationic ion concentrations in freshwater. Regarding the first hypothesis, the contribution of CsPMs was not sufficient to explain the high K_d values observed for FDNPP-derived ^{137}Cs in freshwater (Konoplev et al., 2016; Miura et al., 2018). The second hypothesis is more reliable because the concentrations of monovalent cationic ions in the irrigation waters are low as follows: Cs^+: 0.011–0.7 nM, Na^+: 0.038–0.31 mM, K^+: 0.0057–0.26 mM, and NH_4^+: <0.008–0.037 mM (Tsukada et al., 2017). The chemical model suggests that the concentrations of stable Cs^+ ions and coexisting cationic ions directly affect the K_d level, as shown in Appendix Eqs. (16) and (17).

Considering that the SS concentrations in irrigation waters ranged from 7.8×10^{-7} to 5.7×10^{-5} kg L^{-1}, the binding site concentrations in irrigation waters estimated from the lower and upper lines were 0.78–58 pmol L^{-1} and 0.025–1.8 nmol L^{-1}, respectively. Possibly, most of the binding sites of Cs in the SS are occupied by ^{133}Cs, considering that the ^{137}Cs concentrations in the SS of the irrigation waters ranged from 1.5 to 300 pmol kg^{-1} (6.6×10^3–1.3×10^5 Bq kg^{-1}). The hypothesis that most of the binding sites of Cs in the SS are occupied by stable Cs is supported by the fact that the ^{137}Cs concentrations in the SS were almost constant, even in storm flow, though enhanced dissolved ^{137}Cs concentrations in river waters were observed under storm flow conditions compared to those under base flow conditions (Tsuji et al., 2016). These findings suggest that the major chemical process controlling ^{137}Cs in the irrigation waters is the isotope exchange reaction between ^{133}Cs and ^{137}Cs under low-K conditions, instead of a metal exchange reaction. However, to explain causes of the enhanced dissolved ^{137}Cs river waters under the storm condition, we propose possible two chemical mechanisms: 1. Metal exchange reaction by enhanced K^+, and 2. Increase of dissolved stable Cs, including the formation of colloidal particles having Cs binding site. It is noteworthy that a level of dissolved stable Cs in fresh waters is not primarily governed by dissolution equilibrium of that in SS: ex. sea salt is a potential source of stable Cs in fresh waters, which may be supplied by Typhoon. Therefore, measurements of the dissolved stable Cs and K, as well as their chemical speciation, are important to better understand behaviors of dissolved ^{137}Cs under the storm conditions. In marine environments, the interaction of ^{137}Cs between the dissolved and sediment phases may be governed by the isotope exchange reactions between ^{133}Cs and ^{137}Cs, as in fresh water (Hirose and Povinec, 2023).

The chemical interactions of alkali metal ions with organic matter (ligands) are generally weak, characterized by the stability constants of metal complexes with organic ligands (Hirose and Povinec, 2022). For example, the stability constants of metal complexes with ethylenediamine tetraacetic acid (EDTA), a typical chelating reagent, are in the following order: Cs^+(log K_{ML}: 0.15) < K^+(log K_{ML}: 0.8) < Na^+(log K_{ML}: 1.66) ≪ Sr^{2+}(log K_{ML}: 8.63) < Ca^{2+}(log K_{ML}: 10.96) ≪ Cu^{2+}(log K_{ML}: 18.8) ≪ Fe^{3+}(log K_{ML}: 25.1). It is well known that macrocyclic polyethers (crown ethers) form relatively stable complexes with alkali metal ions. The stability constants of Cs complexes with 1,4,7,10,13,16-hexaoxacyclo-octadecane are $10^{\circ.96}$ in a water medium and $10^{4.6}$ in a methanol medium (Arnaud-Neu et al., 2003; Makrlík et al., 2010). These findings show that the Cs complex with a naturally strong binding site in the river system was extremely stable compared to those with known organic ligands. The chemical model suggests that there is no evidence of the presence of organic binding sites interacting with Cs^+ with a K_d value greater than 10^3. Notably, the K_d value is the product of the stability constant of the Cs–SS complex and binding site concentration in the SS (Appendix Eq. (15)). The model also revealed that the stable Cs concentration in natural water is a key factor controlling the K_d values. To elucidate the organic binding sites in SS of freshwater, it may be important to examine the relationship between the K_d values and ^{133}Cs concentration in the aqueous phase under conditions of higher ^{133}Cs concentrations (>1 nmol L^{-1}).

In case when the partition coefficients of metal ions are generally governed by chemical thermodynamics, the partition coefficients are closely related to temperature and pressure (Stumm and Morgan, 2012). If the partition coefficient of ^{137}Cs reflects that of ^{133}Cs because of the isotope exchange equilibrium between ^{133}Cs and ^{137}Cs, the K_d of ^{137}Cs is a function of temperature and pressure. Hirose and Povinec (2023) revealed that the logarithmic K_d values of ^{137}Cs between overlying water and sediment in the Sea of Japan were linearly related to water depth (equal to pressure). Furthermore, Tsuji et al. (2023) suggested that temperature is an important parameter for the K_d values of ^{137}Cs in shallow fresh waters, according to chemical thermodynamics.

3.3. Effects of SS concentration

The chemical model suggests that it is essential to clarify the binding-site concentrations of SS and colloids in natural waters to gain a better understanding of the factors controlling the partition coefficients of ^{137}Cs (Appendix Eqs. (17) and (19)). However, the chemical and mineralogical properties of SS in natural waters are complex and involve mineral particles and organic matter (e.g., living and non-living microorganisms and detrital matter). The effects of the SS concentration on dissolved and suspended ^{137}Cs in natural waters cannot be predicted from the present chemical model because of limited information on the binding site in SS. However, enhanced dissolved ^{137}Cs concentrations in river waters were observed under storm flow conditions compared to those under base flow conditions (Tsuji et al., 2016), in which the dissolved ^{137}Cs concentrations increased with increasing SS concentrations in river water. Therefore, it is important to examine the relationships between the SS concentrations and dissolved and suspended ^{137}Cs concentrations in natural waters, as well as the dissolved ^{133}Cs concentrations.

To elucidate the relationship between K_d and SS concentrations in natural waters, log-log plots between K_d and SS concentrations were constructed for the river and irrigation waters in Fukushima Prefecture. The results are shown in Fig. 6. The log K_d values were broadly correlated with the log SS concentration in rivers (Fig. 6A) (correlation slope: -0.10 ± 0.16, intercept: 5.58 ± 0.41, correlation factor: 0.48). A similar correlation was observed for the irrigation waters (Fig. 6B) (correlation slope: -0.61 ± 0.16, intercept: 5.75 ± 0.23, correlation factor: 0.48).

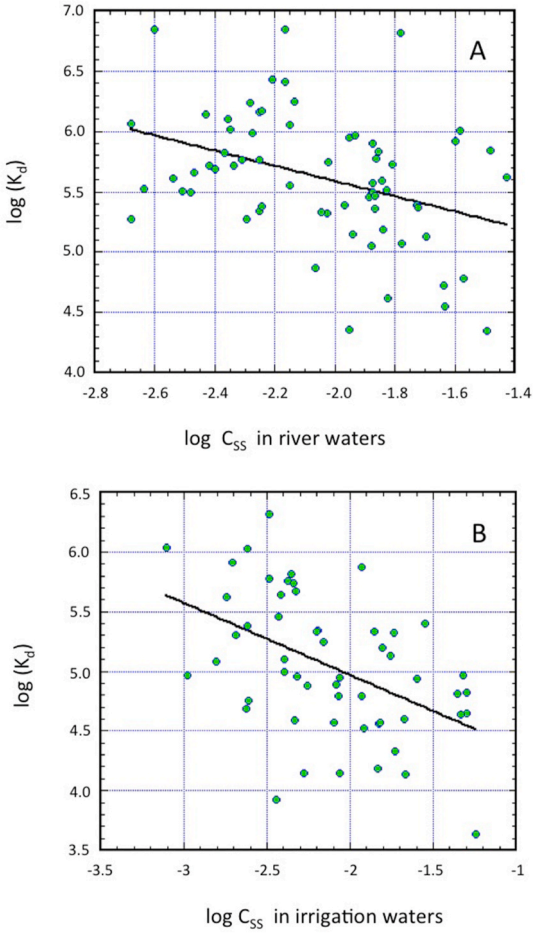

Fig. 6. Relationship between the partition coefficient and concentrations of suspended sediment in (A) river waters and (B) irrigation waters (C_{SS}). Unit: kg L^{-1} (K_d), g L^{-1} (C_{SS}). The solid line shows the correlation curve.

Boyer et al. (2018) reported that the correlation slope of the log-log plots between K_d and the SS concentration in fresh water was −0.49. If the binding site for ^{137}Cs in colloidal and suspended matter exists on the particle surface, the slope of Appendix Eq. (19) is expected to be −2/3 instead of −1 owing to the first approximation of the volume–surface relationship. To verify this hypothesis, we examined the effects of the SS particle size in river water. The median diameter of SS in the river waters of Fukushima Prefecture ranged from 5.5 to 48.6 μm. We introduced new variables, including the particle size of SS, that is, the total surface area of SS in the river waters, S_{tss} (kg L^{-1} m^{-1}) and the area-based partition coefficient for SS, $K_{d(S),Cs,ss}$ (m L kg^{-1}). S_{tss} and $K_{d(S),Cs,ss}$ are defined as follows:

$$S_{tss} = C_{ss}/d_{ss}$$

$$K_{d(s),Cs,ss} = C_{Cs,ss,w}/(C_{Cs,d} \times S_{tss}) \quad (4)$$

where d_{ss} denotes the median value of the particle diameter of the SS. The log-log plot between S_{tss} and $K_{d(s),Cs,ss}$ is shown in Fig. 7. The log $K_{d(s),Cs,ss}$ value was correlated with the logarithm of the total surface area of SS in river water (correlation slope: -0.71 ± 0.17; intercept: 3.60 ± 0.08; correlation factor: 0.46). Although the correlation factor and absolute value of the slope for the log-log plots between $K_{d(s),Cs,ss}$ and S_{tss} are larger than those between K_d and C_{ss}, the absolute correlation slope remains smaller than the theoretical value (−1). The results suggest that the presence of colloidal ^{137}Cs plays an important role in controlling the K_d values in river water and that the particle size of SS in river water is an essential factor for controlling the K_d of ^{137}Cs in river systems. However, little information is available on the chemical and physical properties of colloidal Cs or the relationship between colloidal and suspended Cs.

Finally, we discussed the relationships between SS and dissolved metals (K and ^{133}Cs) in irrigation waters. The log-log plots of SS and K concentrations in irrigation waters was examined (Supplementary Fig. 5S). The result revealed no correlation between SS and K concentration (slope: 0.016 ± 0.111, intercept: -4.8 ± 0.2, correlation factor: 0.02. The log-log plots of the SS and ^{133}Cs concentrations in the irrigation waters was also carried out (Supplementary Fig. 6S). The result revealed that a weak positive correlation occurred between the logarithmic SS and logarithmic ^{133}Cs concentrations in the irrigation waters (slope: 0.29 ± 0.11, intercept: -9.68 ± 0.23, correlation factor: 0.35). The negative correlation between the SS concentration and K_d value in the irrigation waters may be explained by the enhanced dissolved ^{133}Cs concentration in high SS concentration. However, it is unknown why the enhanced dissolved ^{133}Cs concentration occurs in the higher SS

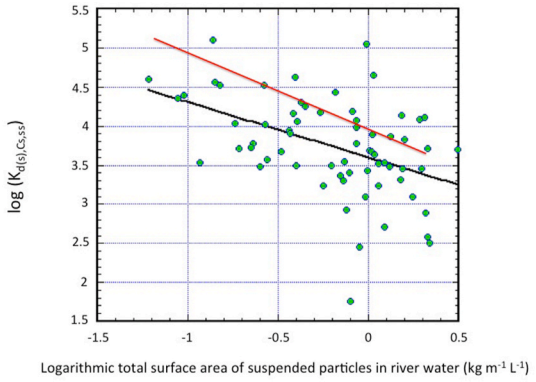

Fig. 7. Relationship between the area-base partition coefficient (unit: m L kg^{-1}) and total surface area of suspended sediment particles in the river water (unit: kg m^{-1} L^{-1}). Black and red solid lines represent the correlation curve and curve of slope of unity, respectively. (For interpretation of the references to colour in this figure legend, the reader is referred to the Web version of this article.)

concentration in the irrigation waters.

4. Conclusion

After the FDNPP accident, the MOE monitored the radioactivity in freshwater systems (e.g., rivers, ponds) to assess the environmental effects of FDNPP-derived radionuclides. We analyzed radioactivity data from a river system in Fukushima Prefecture, Japan, using the partition coefficient of ^{137}Cs between the suspended and dissolved phases, K_d, as a tool to understand the dynamic behavior of ^{137}Cs in natural water systems. It is important to reveal the factors controlling the partition coefficient of ^{137}Cs in natural water systems because the partition coefficient of FDNPP-derived ^{137}Cs in freshwater (e.g., rivers, ponds) showed larger spatial variability. The partition coefficient of ^{137}Cs in river water was related to EC, with the log K_d values negatively correlated with the log EC values, except those in the irrigation waters in Fukushima. The partition coefficient of ^{137}Cs in rivers is also related to the concentration of SS, and there is a broad correlation between the log K_d values and the log SS concentration in river water. We developed a chemical model to explain the relationship between the K_d values and EC (or SS concentration). The chemical model requires that the total ^{133}Cs, the major cesium isotope in the environment, plays an essential role in the partitioning of Cs between the dissolved and suspended phases, in which isotope exchange reactions between ^{133}Cs and ^{137}Cs occur between the different phases. The chemical model suggests that the partition coefficient of ^{137}Cs in natural waters is inversely related to the concentrations of competing ions such as K^+ and/or coexisting $^{133}Cs^+$. According to the analysis of irrigation water data (Tsukada et al., 2017), log K_d values were negatively correlated with the log ^{133}Cs concentrations with a slope of −1, whereas there was no correlation between the log K_d values and the log K^+ concentration. This relationship was established for coastal sediments. These findings suggest that most of the binding sites in SS are occupied by ^{133}Cs, and that the major chemical process in natural water systems is the isotope exchange reaction between ^{133}Cs and ^{137}Cs, instead of the metal ion exchange reaction with K^+. The chemical model requires the measurement of dissolved and suspended ^{133}Cs, as does their chemical speciation including colloids, in natural waters, similar to ^{137}Cs measurements, to better understand the migration behavior of ^{137}Cs in terrestrial environments. Especially, it is important to better understand factors (sources, transport and others) controlling ^{133}Cs in natural waters. The present chemical model cannot solve several problems from the limited observation data. One is the characterization of the chemical property of the binding sites in suspended particles, such as whether two types of binding sites coexist, although it is likely that one of the strong binding sites is characterized as an FES of clay minerals.

CRediT authorship contribution statement

Katsumi Hirose: Conceptualization, Funding acquisition, Investigation, Visualization, Writing – original draft. **Yuichi Onda:** Conceptualization, Data curation, Funding acquisition, Investigation, Project administration, Supervision. **Hirofumi Tsukada:** Conceptualization, Data curation, Investigation. **Yuko Hiroyama:** Investigation. **Yukiko Okada:** Investigation. **Yoshikazu Kikawada:** Conceptualization, Investigation.

Declaration of competing interest

The authors declare that they have no known competing financial interests or personal relationships that could have appeared to influence the work reported in this paper.

Data availability

Data will be made available on request.

Acknowledgments

The authors are indebted to numerous colleagues of MOE for sampling and analyzing river water samples in Fukushima Prefecture. This work was supported by ERAN P-23-03, University of Tsukuba, Japan and Grant-in-Aid for Scientific Research (A) 22H00556, Japan.

Appendix A. Supplementary data

Supplementary data to this article can be found online at https://doi.org/10.1016/j.jenvrad.2024.107486.

Appendix

Chemical equilibrium model

The chemical equilibrium model (Stumm and Morgan, 2012) is effective for revealing the chemical reactions of metal ions in solution, including those in the solid phase, such as suspended matter and bottom sediments. In this study, we assumed that the chemical reactions of Cs^+, including the complexation of Cs^+ with mineral and organic binding sites, metal exchange reactions, and presence of colloidal species, are established in natural water systems (Fig. A1). Cs sorption kinetics experiments revealed that the sorption equilibrium for FES (initial Cs concentration = 0.16 nM) is reached within one month (Poinssot et al., 1999). In natural water systems, the chemical equilibrium model should be described using stable cesium (^{133}Cs) concentrations, as all chemical reactions are governed by stable cesium ions owing to the high mass abundance of stable cesium within cesium isotopes. This hypothesis is supported by the finding that the concentrations of stable isotope ^{133}Cs dissolved in the river and pond waters of Fukushima Prefecture were in the range of 10–700 pmol L^{-1} (Tsukada et al., 2017), whereas the mass concentrations of ^{134}Cs and ^{137}Cs dissolved in fresh water were less than 0.02 pmol L^{-1} (~10 Bq L^{-1} of ^{137}Cs).

The thermodynamic partition coefficient between dissolved and suspended Cs, $K_{d,Cs,ss}$ in natural water is expressed as follows:

$$K_{d,Cs,ss} = C_{Cs,ss}/C_{Cs,d} \quad (1)$$

where $C_{Cs,ss}$ and $C_{Cs,d}$ denote the total Cs concentration in SS (mol kg^{-1}) and total dissolved Cs concentration in natural water (mol L^{-1}), respectively. The thermodynamic partition coefficient of stable Cs (^{133}Cs) corresponds to that of exchangeable ^{133}Cs ($^{133}Cs_{ex}$). When an isotope exchange equilibrium between $^{133}Cs_{ex}$ and ^{137}Cs is established in a natural water system, the partition coefficient of ^{137}Cs should coincide with that of $^{133}Cs_{ex}$, as the $^{137}Cs/^{133}Cs_{ex}$ ratio in the dissolved phase is equal to that in SS. Notably, the concentration of $^{133}Cs_{ex}$ in SS was larger than the ^{137}Cs concentration, although the exchangeable fraction of ^{133}Cs was less than 3% of the total ^{133}Cs content in the soil (Hirose et al., 2015; Kikawada et al., 2015), and FDNPP-derived ^{137}Cs partly contained ^{137}Cs refractory particles, such as Cs hot particles (Adachi et al., 2013; Hirose, 2020; Igarashi et al., 2019; Miura

et al., 2018).

We now consider the metal complexation between Cs^+ and the binding sites (or ligands) in the colloidal matter and SS, L_{col} and L_{ss} (Fig. A1a). In this case, it is postulated that two types of binding sites, which may include a strong (mineral) binding site ($L_{col,1}$ and $L_{ss,1}$) and a weak (organic or planar) binding site ($L_{col,2}$ and $L_{ss,2}$), coexist in natural water.

Colloidal complex: $Cs^+ + L_{col,i} = CsL_{col,i}$ 2

SS complex: $Cs^+ + L_{ss,i} = CsL_{ss,i}$ 3

$i = 1,2$.

The corresponding stability constants $K_{Cs,col,i}$ and $K_{Cs,ss,i}$ are expressed as

$$K_{Cs,col,i} = [CsL_{col,i}]/([Cs^+][L_{col,i}]) \quad (4)$$

$$K_{Cs,ss,i} = [CsL_{ss,i}]/([Cs^+][L_{ss,i}]) \quad (5)$$

where $[CsL_{col,i}]$ and $[CsL_{ss,i}]$ are the Cs concentrations associated with binding site i in the colloid and SS, respectively, and $[Cs^+]$ is the free Cs^+ ion concentration in natural water.

Generally, the binding sites in colloidal matter and SS can react with cationic ions other than Cs, in which potassium and ammonium ions are candidates as exchangeable cationic ions, though protons and many other metal ions are postulated to be potential cationic ions because of the anionic nature of binding sites.

Colloidal complex: $M^{n+} + L_{col,i} = ML_{col,i}$ 6

Suspended complex: $M^{n+} + L_{ss,i} = ML_{ss,i}$ 7

The corresponding stability constants for the formation of $ML_{col,i}$ and $ML_{ss,i}$ are expressed as

$$K_{M,col} = [ML_{col,i}]/([M^{n+}][L_{col,i}]) \quad (8)$$

$$K_{M,ss} = [ML_{ss,i}]/([M^{n+}][L_{ss,i}]) \quad (9)$$

The total dissolved Cs concentration in natural water, including colloidal Cs, and the suspended Cs concentration in natural water are expressed as follows:

$$C_{Cs,d} = [Cs^+] + \Sigma\left[CsL_{col,i}\right] = [Cs^+] + \Sigma K_{Cs,col,i}[Cs^+]\left[L_{col,i}\right] = [Cs^+]\left(1+\Sigma K_{Cs,col,i}\left[L_{col,i}\right]\right) = [Cs^+]\alpha_{Cs,col,i}$$
$$C_{Cs,ss} = \Sigma\left[CsL_{ss,i}\right] \quad (10)$$

where $\alpha_{Cs,col,i}$ denotes the side reaction coefficient of dissolved Cs in colloidal matter, $\alpha_{Cs,col,i} = 1 + \Sigma K_{Cs,col,i}[L_{col,i}]$.

The binding site concentrations in colloidal matter and SS are expressed as follows:

$$C_{L,col,i} = \left[L_{col,i}\right] + \left[CsL_{col,i}\right] + \Sigma\left[ML_{col,i}\right]$$
$$= \left[L_{col,i}\right]\left(1 + K_{Cs,col,i}\left[Cs^+\right] + \Sigma K_{M,col,i}[M^{n+}]\right) = \left[L_{col,i}\right]\left(\alpha_{L,col,i} + K_{Cs,col,i}\left[Cs^+\right]\right) \quad (11)$$

$$C_{L,ss,i} = \left[L_{ss,i}\right] + \left[CsL_{ss,i}\right] + \Sigma\left[ML_{ss,i}\right]$$
$$= \left[L_{ss,i}\right]\left(1 + K_{Cs,ss,i}\left[Cs^+\right] + \Sigma K_{M,ss,i}[M^{n+}]\right) = \left[L_{ss,i}\right]\left(\alpha_{L,ss,i} + K_{Cs,ss,i}\left[Cs^+\right]\right) \quad (12)$$

where $\alpha_{L,col,i}$ and $\alpha_{L,ss,i}$ denote the side reaction coefficients of binding sites in colloidal matter and SS, respectively, $\alpha_{L,col,i} = 1 + \Sigma K_{M,col,i}[M^{n+}]$ and $\alpha_{L,ss,i} = 1 + \Sigma K_{M,ss,i}[M^{n+}]$.

Generally, the partition coefficients can be written using the binding site concentrations as follows:

$$K_{d,Cs,ss} = C_{Cs,ss,w}/C_{Cs,d}$$
$$= \Sigma\left(K'_{Cs,ss,i}C_{L,ss,i}\right)/\left\{\alpha_{Cs,col,i}\left(1 + K'_{Cs,ss,i}[Cs^+]\right)\right\} \quad (13)$$

where $K'_{Cs,ss,i}$ is a conditional equilibrium constant that includes the effects of competitive ions, $K'_{Cs,ss,i} = K_{Cs,ss,i}/\alpha_{L,ss,i}$.

Presence of only one binding site in SS.

As Eq. (13) is too complicated to yield an understanding of the chemical processes between the dissolved and suspended phases, we postulate that a single binding site (strong ligand) is related to the association with Cs ions. In this case, Eq. (13) can be simplified as follows:

$$K_{d,Cs,ss} = (K'_{Cs,ss,1}C_{L,ss,1})/\{\alpha_{Cs,col,1}(1 + K'_{Cs,ss,1}[Cs^+])\} \quad (14)$$

To understand the major chemical processes that occur in natural systems, we considered two extreme cases. The first extreme case is that most of the dissolved Cs exists in ionic form (Cs^+), $\alpha_{L,col,1} = 1$ (or $1 > \Sigma K_{M,col,i}[M^{n+}]$). There is no information on the chemical states of the binding sites in the SS. Most binding sites in the SS are occupied by metal ions, such as K^+, when Cs is a minor component: $1 > K_{Cs,ss,1}/\alpha_{L,ss,1}[Cs^+]$. Eq. (14) can be simplified as follows:

$$K_{d,Cs,ss} = K'_{Cs,ss,1}\, C_{L,ss,1} \quad (15)$$

Now, we assume that most of the binding sites in the SS are occupied by metal ions such as M^{n+}. We obtain the following simple equation:

$$K_{d,Cs,ss} = K_{Cs,ss,1}\, C_{L,ss,1} / (\, K_{M,ss,1}[M^{n+}]) \\ \text{or } log(K_{d,Cs,ss}) = \log(K_{Cs,ss,1} C_{L,ss,1} / K_{M,ss,1}) - \log[M^{n+}] \quad 16$$

This equation suggests that the partition coefficient of ^{137}Cs between the dissolved and suspended phases is inversely related to the concentration of competing cations such as K^+. In other words, the major chemical process was the metal exchange reaction between ^{137}Cs and cationic metal ions (M^{n+}) in the SS.

When a major part of the binding site in the SS is occupied by stable Cs ($1 < K_{Cs,ss,1}/\alpha_{L,ss,1}[Cs^+]$), we obtain the following equation:

$$K_{d,Cs,ss} = C_{L,ss,1}/[Cs^+] \text{ or } log\,(K_{d,Cs,ss}) = log\,(C_{L,ss,1}) - log\,([Cs^+]) \quad 17$$

This equation suggests that the partition coefficient of ^{137}Cs between the dissolved and suspended phases is inversely related to the stable Cs ion concentration dissolved in natural water, assuming that the portion of the binding site concentration in the SS is almost constant, irrespective of the different environmental conditions of the sampling sites, as shown in Fig. A1b.

In another extreme case, most of the dissolved Cs exists in colloidal form: $1 < K_{Cs,col,1}[L_{col}]$.

$$K_{d,Cs,ss} = \{(K_{Cs,ss,1}C_{L,ss,1}\alpha_{L,col,1})/(K_{Cs,col,1}\, C_{L,col,1})\, \alpha_{L,ss,1}\}/\{(1 + K_{Cs,ss,1}/\alpha_{L,ss,1}[Cs^+])/(1 + K_{Cs,col,1}/\alpha_{L,col,1}[Cs^+])\} \quad 18$$

If the chemical properties of the binding site in the SS are the same as those in the colloidal matter, that is, $K_{Cs,ss,1} = K_{Cs,col,1}$ and $\alpha_{L,col,1} = \alpha_{L,ss,1}$, and the free bonding site concentrations in the SS are negligible compared with the binding sites associated with metal ions, we have a very simple relationship, as follows:

$$K_{d,Cs,ss} = C_{L,ss,1} / C_{L,col,1} \quad 19$$

The chemical model revealed that when colloidal ^{137}Cs exists as a major dissolved species, the partition coefficient between the dissolved and suspended ^{137}Cs is related to the concentration ratio of the suspended binding site to the colloidal binding site in natural water, irrespective of the concentrations of Cs and coexisting cationic ions.

Coexistence of two types of binding sites

We examined the effect of the coexistence of two types of binding sites on the relationship between $K_{d,Cs,ss}$ and Cs concentrations in natural systems using a chemical model. When most of the Cs $^+$ dissolved in natural water exists as free metal ions (Cs^+), Eq. (13) is expressed as follows:

$$K_{d,Cs,ss} = (K'_{Cs,ss,1}C_{L,ss,1})/(1 + K'_{Cs,ss,1}[Cs^+]) + (K'_{Cs,ss,2}C_{L,ss,2})/(1 + K'_{Cs,ss,2}[Cs^+])\} \quad 20$$

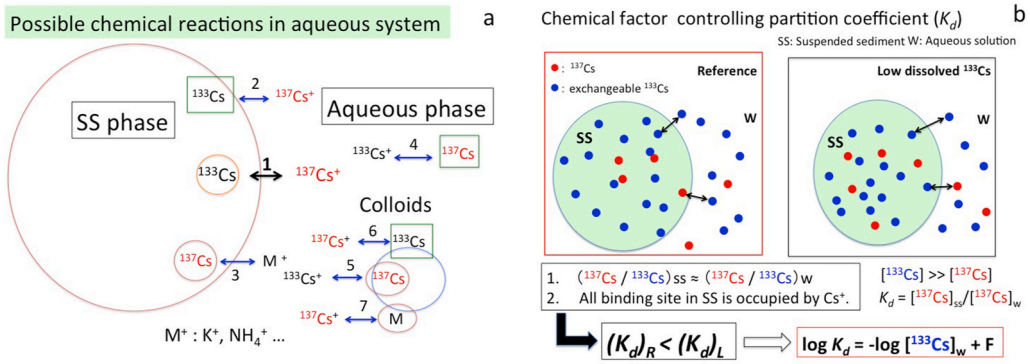

Fig. A1. Scheme of chemical model of partitioning of ^{137}Cs between water and suspended sediment. a. Possible chemical reactions. Black double arrow: major reaction 1 (isotope exchange reaction with strong binding site (mineral site) in SS). Blue double arrows: side reactions 2 (isotope exchange reaction with weak binding site (organic site) in SS), 3 (metal exchange reaction with strong binding site in SS), 4 (isotope exchange reaction with weak binding site in water), 5 (isotope exchange reaction with strong binding site in colloids), 6 (isotope exchange reaction with weak binding site in colloid), and 7 (metal exchange reaction with strong binding site in colloids). b. Model drawing of effect of change of stable Cs in isotope exchange reaction.

References

Adachi, K., Kajino, M., Zaizen, Y., Igarashi, Y., 2013. Emission of spherical cesium-bearing particles from an early stage of the Fukushima nuclear accident. Sci. Rep. 3, 2554. https://doi.org/10.1038/srep02554.

Arnaud-Neu, F., Delgado, R., Chaves, S., 2003. Critical evaluation of stability constants and thermodynamic functions of metal complexes of crown ethers. Pure Appl. Chem. 76, 71–102.

Beneš, P., Černík, M., Lam Ramos, P., 1992. Factors affecting interaction of radiocesium with freshwater solids. II. Contact time, concentration the solid and temperature. J. Radioanal. Nucl. Chem. 159, 201–218.

Beneš, P., Lam Romos, P., Poliak, R., 1989. Factors affecting of radiocesium with freshwater solids. J. Radioanal. Nucl. Chem. 133 (1), 359–376.

Boyer, P., Wells, C., Howard, B., 2018. Extended K_d distributions for freshwater environment. J. Environ. Radioact. 192, 128–142. https://doi.org/10.1016/j.jenvrad.2018.06.006.

Brouwer, E., Baeyens, B., Maes, A., Cremers, A., 1983. Cesium and rubidium ion equilibriums in illite clay. J. Phys. Chem. 87, 1213–1219. https://doi.org/10.1021/j100230a024.

Chester, R., 2003. Marine Geochemistry. Blackwell Science, p. 505.

Comans, R.N.J., Middelburg, J.J., Zonderhuis, J., Woittiez, J.R.W., Lange, G.J.D., Das, H. A., Weijden, C.H.V.D., 1989. Mobilization of radiocaesium in pore water of lake sediments. Nature 339, 367–369. https://doi.org/10.1038/339367a0.

Duursma, E.K., Eisma, D., 1973. Theoretical, experimental and field studies concerning reactions of radioisotopes with sediments and suspended particles of the sea Part C: applications to field studies. Neth. J. Sea Res. 6, 265–324.

Eyrolle, F., Charmasson, S., 2001. Distribution of organic carbon, selected stable elements and artificial radionuclides among dissolved colloidal and particulate

phases in the Rhone River (France): preliminary results. J. Environ. Radioact. 55, 145–155. https://doi.org/10.1016/s0265-931x(00)00188-0.
Eyrolle-Boyer, F., Boyer, P., Garcia-Sanchez, L., Métivier, J.M., Onda, Y., De Vismes, A., Cagnat, X., Boulet, B., Cossonnet, C., 2016. Behaviour of radiocaecium in coastal rivers of the Fukushima Prefecture (Japan) during the conditions of low flow and low turbidity – insight on the possible role of small particles and detrital organic compounds. J. Environ. Radioact. 151, 328–340. https://doi.org/10.1016/j.jenvrad.2015.10.028.
Funaki, H., Tsuji, H., Nakanishi, T., Yoshimura, K., Sakuma, K., Hayashi, S., 2022. Remobilisation of radiocaesium from bottom sediments to water column in reservoirs in Fukushima. Japan. Sci. Total Environ. 812, 152534 https://doi.org/10.1016/j.scitotenv.2021.152534.
Gustafsson, C., Gschwend, P.M., 1997. Aquatic colloids: concepts, definitions, and current challenges. Limnol. Oceanogr. 42, 519–528. https://doi.org/10.4319/lo.1997.42.3.0519.
Higgo, J.J.W., Rees, L.V.C., 1986. Adsorption of actinides by marine sediments: effect of the sediment/seawater ratio on the measured distribution ratio. Environ. Sci. Technol. 20, 483–490. https://doi.org/10.1021/es00147a007.
Hirayama, Y., Okawa, A., Nakamachi, K., Aoyama, T., Okada, Y., Oi, T., Hirose, K., Kikawada, Y., 2020. Estimation of water seepage rate in the active crater lake system of Kusatsu–Shirane volcano, Japan, using FDNPP-derived radioactive cesium as a hydrological tracer. J. Environ. Radioact. 218, 106257 https://doi.org/10.1016/j.jenvrad.2020.106257.
Hirose, K., 2020. Atmospheric effects of Fukushima nuclear accident: a review from a sight of atmospheric monitoring. J. Environ. Radioact. 218, 106240 https://doi.org/10.1016/j.jenvrad.2020.106240.
Hirose, K., Aoyama, M., Sugimura, Y., 1990. Plutonium and cesium isotopes in river waters in Japan. J. Radioanal. Nucl. Chem. Artic. 141, 191–202. https://doi.org/10.1007/BF02060198.
Hirose, K., Povinec, P.P., 2022. Ten years of Investigations of Fukushima radionuclides in the environment: a review on process studies in environmental compartments. J. Environ. Radioact. 251–252, 106929 https://doi.org/10.1016/j.jenvrad.2022.106929.
Hirose, K., Povinec, P.P., 2023. Temporal changes of ^{137}Cs concentrations in the Far Eastern Seas: partitioning of ^{137}Cs between overlying water and sediments. Sci. Rep. 13, 22963 https://doi.org/10.1038/s41598-023-49083-4.
Hirose, M., Kikawada, Y., Tsukamoto, A., Oi, T., Honda, T., Hirose, K., Takahashi, H., 2015. Chemical forms of radioactive Cs in soils originated from Fukushima Dai-ichi nuclear power plant accident studied by extraction experiments. J. Radioanal. Nucl. Chem. 303, 1357–1359. https://doi.org/10.1007/s10967-014-3592-1.
Honeyman, B.D., Santschi, P.H., 1988. Metals in aquatic systems. Predicting their scavenging residence times from laboratory data remains a challenge. Environ. Sci. Technol. 22, 862–871. https://doi.org/10.1021/es00173a002.
IAEA, 1994. Handbook of Parameter Values for the Prediction of Radionuclide Transfer in Temperate Environments. International Atomic Energy Agency, Vienna. Technical Report Series. IAEA-Trs 364.
IAEA, 2010. Handbook of Parameter Values for the Prediction of Radionuclide Transfer in Terrestrial and Freshwater Environments. International Atomic Energy Agency, Vienna. Technical Report Series. IAEA-Trs 472.
Igarashi, Y., Kogure, T., Kurihara, Y., Miura, H., Okunuma, T., Satou, Y., Takahashi, Y., Yamazaki, N., 2019. A review of Cs-bearing microparticles in the environment emitted by Fukushima Dai-ichi Nuclear Power Plant accident. J. Environ. Radioact. 205–206, 101–118. https://doi.org/10.1016/j.jenvrad.2019.04.011.
Iwagami, S., Tsujimura, M. Onda, Nishino, M., Konuma, R., Nishino, M., Abe, Y., Hada, M., Pun, I., Sakaguchi, A., Kondo, H., Yamamoto, M., Miyata, Y., Igarashi, Y., 2017a. Temporal changes in dissolved ^{137}Cs concentration in groundwater and stream water in Fukushima after the Fukushima Dai-ichi Nuclear Power Plant accident. J. Environ. Radioact. 166, 458–465. https://doi.org/10.1016/j.jenvrad.2016.07.025.
Iwagami, S., Onda, Y., Tsujimura, M., Abe, Y., 2017b. Contribution of radioactive ^{137}Cs discharge by suspended sediment, coarse organic matter, and dissolved fraction from a headwater catchment in Fukushima after the Fukushima Dai-ichi Nuclear Power Plant accident. J. Environ. Radioact. 166, 466–474. https://doi.org/10.1016/j.jenvrad.2016.07.025.
Iwagami, S., Onda, Y., Sakashita, W., Tsujimura, M., Satou, Y., Konuma, R., Nishino, M., Abe, Y., 2019a. Six-year monitoring study of ^{137}Cs discharge from headwater catchments after the Fukushima Dai-ichi Nuclear Power Plant accident. J. Environ. Radioact. 210, 106001 https://doi.org/10.1016/j.jenvrad.2019.106001.
Iwagami, S., Tsujimura, M., Onda, Y., Konuma, R., Satou, Y., Sakakibara, K., Yoschenko, V., 2019b. Dissolved ^{137}Cs concentrations in stream water and subsurface water in a forested headwater catchment after the Fukushima Dai-ichi Nuclear Power Plant accident. J. Hydrol. 573, 688–696. https://doi.org/10.1016/j.jhydrol.2019.04.019.
Kawano, T., Onda, Y., Kato, H., Takahashi, J., 2023. Mechanisms of 137Cs leaching based on long-term observations in forested headwater catchments in Yamakiya, Fukushima Prefecture, Japan. Sci. Total Environ. https://doi.org/10.1016/j.scitotenv.2023.167837.
Kikawada, Y., Hirose, M., Tsukamoto, A., Nakamachi, K., Oi, T., Honda, T., Takahashi, H., Hirose, K., 2015. Mobility of radioactive cesium in soil originated from the Fukushima Daiichi nuclear disaster: application of extraction experiments. J. Radioanal. Nucl. Chem. 304, 27–31. https://doi.org/10.1007/s10967-014-3713-x.
Konoplev, A., Golosov, V., Laptev, G., Nanba, K., Onda, Y., Takase, T., Wakiyama, Y., Yoshimura, K., 2016. Behavior of accidently released radiocesium in soil-water environment: looking at Fukushima from a Chernobyl perspective. J. Environ. Radioact. 151, 568–578. https://doi.org/10.1016/j.jenvrad.2015.06.019.
Kusakabe, M., Takata, H., 2020. Temporal trends of ^{137}Cs concentration in seawaters and bottom sediments in coastal waters around Japan: implication of the K_d concept in the dynamic marine environment. J. Radioanal. Nucl. Chem. 323, 567–580. https://doi.org/10.1007/s10967-019-06958-z.
Lagaly, G., 2006. Colloid clay science. Develop. Clay Sci. 1, 141–245. https://doi.org/10.1016/S1572-4352(05)01005-6.
Madruga, M.J., Vaz Carreiro, M.C., Bettencourt, A.O., 1988. Experimental study of ^{134}Cs behavior in freshwater sediments. Impact Accidents d'origine nucléaire sur l'environment, IVe Symp. Intern. de Radioecologie de Cadarache 1, C51–C59.
Makrlík, E., Vañura, P., Selucký, P., 2010. Distribution of microamounts of cesium in the two-phase water-HCl-nitrobenzene-2,3-naphtho-15-crown-5-hydrogen dicarbollylcobaltate extraction system. Acta Chim. Slov. 57, 470–474.
Mansfeld, A., 1980. Methodology used for the study of sorption properties of bottom sediments and some basic information on the behavior of selected radionuclides in aqueous media. In: International Studies on the Radioecology of the Danube River 1976-1979, p. 41. Report IAEA-TECDOC-229. Vienna.
Matsunaga, T., Amano, H., Yanase, N., 1991. Discharge of dissolved and particulate ^{137}Cs in the kuji river Japan. Appl. Geochem. 6, 159–167. https://doi.org/10.1016/0883-2927(91)90026-L.
McKinley, J.P., Zachara, J.M., Heald, S.M., Dohnalkova, A., Newville, M.G., Sutton, S.R., 2004. Microscale distribution of cesium sorbed to biotite and muscovite. Environ. Sci. Technol. 38, 1017–1023. https://doi.org/10.1021/es034569m.
Miura, H., Kurihara, Y., Sakaguchi, A., Tanaka, K., Yamaguchi, N., Higaki, S., Takahashi, Y., 2018. Discovery of radiocesium-bearing microparticles in river water and their influence on the solid-water distribution coefficient (K_d) of radiocesium in the Kuchiboso River in Fukushima. Geochem. J. 52, 145–154. https://doi.org/10.2343/geochemj.2.0517.
MOE (Ministry of the Environment), 2018. Results of Monitoring of Radioactive Materials in Aqueous Environment.
Morel, F.M.M., Gschwend, P.M., 1987. The role of colloids in the partitioning of solutes in natural waters. In: Stumm, W. (Ed.), Aquatic Surface Chemistry. Wiley, pp. 405–422.
Nagao, S., Kanamori, M., Ochiai, S., Inoue, M., Yamamoto, M., 2015. Migration behavior of ^{134}Cs and ^{137}Cs in the niida River water in Fukushima prefecture, Japan during 2011–2012. J. Radioanal. Nucl. Chem. 303, 1617–1621. https://doi.org/10.1007/s10967-014-3686-9.
Nagao, S., Kanamori, M., Ochiai, S., Tomihara, S., Fukushi, K., Yamamoto, M., 2013. Export of ^{134}Cs and ^{137}Cs in the Fukushima River systems at heavy rain by typhoon roke in september 2011. Biogeosciences 10, 6215–6223. https://doi.org/10.5194/bg-10-6215-2013.
Nakao, A., Thiry, Y., Funakawa, S., Kosaki, T., 2008. Characterization of the frayed edge site of micaceous minerals in soil clays influenced by different pedogenetic conditions in Japan and northern Thailand. Soil Sci. Plant Nutr. 54, 479–489. https://doi.org/10.1111/j.1747-0765.2008.00262.x.
Nyléna, T., Grip, H., 1997. The origin and dynamics of ^{137}Cs discharge from a coniferous forest catchment. J. Hydrol. (Wellingt. North) 192, 338–354. https://doi.org/10.1016/S0022-1694(96)03083-1.
Ochiai, S., Ueda, S., Hasegawa, H., Kakiuchi, H., Akata, N., Ohtsuka, Y., Hisamatsu, S., 2015. Effects of radiocesium inventory on ^{137}Cs concentrations in river waters of Fukushima, Japan, under base-low conditions. J. Environ. Radioact. 144, 86–95. https://doi.org/10.1016/j.jenvrad.2015.03.005.
Okumura, M., Kerisit, S., Boura, I., Lammers, L.N., Ikeda, T., Sassi, M., Rosso, K.M., Machida, M., 2018. Radiocesiu interaction with clay mineral: theory and simulation advances Post-Fukushima. J. Environ. Radioact. 189, 135–145. https://doi.org/10.1016/j.jenvrad.2016.03.011.
Onda, Y., Taniguchi, K., Yoshimura, K., Kato, H., Takahashi, J., Wakiyama, Y., Coppin, F., Smith, H., 2020. Radionuclides from the Fukushima Daiichi nuclear power plant in terrestrial systems. Nat. Rev. Earth Environ. 1, 644–660. https://doi.org/10.1038/s43017-020-0099-x.
Osawa, K., Nonaka, Y., Nishimura, T., Tanoi, K., Matsui, H., Mizogichi, M., Tatsuno, T., 2018. Quantification of dissolved and particulate radiocesium fluxes in two rivers draining the main radioactive pollution plume in Fukushima, Japan (2013–2016). Anthropocene 22, 40–50. https://doi.org/10.1016/j.ancene.2018.04.003.
Pinder III, J.E., Hinton, T.G., Whicker, F.W., 2005. The influence of a whole-lake addition of stable cesium on the remobilization of aged ^{137}Cs in a conateminated reservoir. J. Environ. Radioact. 80, 225–243.
Poinssot, C., Baeyens, B., Bradbury, M.H., 1999. Experimental and modelling studies of caesium sorption on illite. Geochem. Cosmochim. Acta 63, 3217–3227. https://doi.org/10.1016/S0016-7037(99)00246-X.
Povinec, P.P., Hirose, K., Aoyama, M., 2013. Fukushima Accident: Radioactivity Impact on the Environment. Elsevier.
Povinec, P.P., Hirose, K., Aoyama, M., Tateda, H., 2021. Fukushima Accident 10 Years after, second ed. Elsevier, p. 559.
Sakaguchi, A., Tanaka, K., Iwatani, H., Chiga, H., Fan, Q., Onda, Y., Takahashi, Y., 2015. Size distribution studies of ^{137}Cs in river water in the Abukuma riverine system following the Fukushima Dai-ichi Nuclear Power Plant accident. J. Environ. Radioact. 139, 379–389. https://doi.org/10.1016/j.jenvrad.2014.05.011.
Sakuma, K., Tsuji, H., Hayashi, S., Funaki, H., Malins, A., Yoshimura, K., Kurikami, H., Kitamura, A., Iijima, K., Hosomi, M., 2018. Applicability of K_d for modelling dissolved ^{137}Cs concentrations in Fukushima river water: case study of the upstream Ota river. J. Environ. Radioact. 184–185, 53–62. https://doi.org/10.1016/j.jenvrad.2018.01.001.
Sawhney, B.L., 1972. Selective sorption and fixation of cations by clay minerals: a review. Clay Clay Miner. 20, 93–100. https://doi.org/10.1346/CCMN.1972.0200208.

Smith, J.T., Comans, R.N.J., Beresford, N.A., Wright, S.M., Howard, B.J., Camplin, W.C., 2000. Chernobyl's legacy in food and water. Nature 405, 141. https://doi.org/10.1038/35012139.

Smith, J.T., Cross, M.A., Wright, S.M., 2002. Predicting transfers of ^{137}Cs in terrestrial and aquatic environments: a whole-ecosystem approach. Radioprotection-Colloq. 37, 37–42.

Stumm, W., Morgan, J.J., 2012. Aquatic Chemistry, Chemical Equilibria and Rates in Natural Water. John Wiley & Sons, Inc., New York.

Takata, H., Aono, T., Aoyama, M., Inoue, M., Kaeriyama, H., Suzuki, S., Tsuruta, T., Wada, T., Wakiyama, Y., 2020. Suspended particle-water interactions increase dissolved ^{137}Cs activities in the nearshore seawater during typhoon Hagibis. Environ. Sci. Technol. 54, 10678–10687. https://doi.org/10.1021/acs.est.0c03254.

Takata, H., Wakiyama, Y., Niida, T., Igarashi, Y., Konoplev, A., Inatomi, N., 2021. Importance of desorption process from Abukuma River's suspended particles in increasing dissolved ^{137}Cs in coastal water during river-flood caused by typhoons. Chemosphere 281, 130751. https://doi.org/10.1016/j.chemosphere.2021.130751.

Taniguchi, K., Onda, Y., Smith, H.G., Blake, W., Yoshimura, K., Yamashiki, Y., Kuramoto, T., Saito, K., 2019. Transport and redistribution of radiocesium in Fukushima fallout through rivers. Environ. Sci. Technol. 53, 12339–12347. https://doi.org/10.1021/acs.est.9b02890.

Trostle, K.D., Ray Runyon, J., Pohlmann, M.A., Redfield, S.E., Pelletier, J., Mcintosh, J., Chorover, J., 2016. Colloids and organic matter complexation control trace metal concentration-discharge relationships in Marshall Gulch stream waters. Water Resour. Res. 52, 7931–7944. https://doi.org/10.1002/2016WR019072.

Tsuji, H., Ishii, Y., Shin, M., Taniguchi, K., Arai, H., Kurihara, M., Yasutaka, T., Kuramoto, T., Nakanishi, T., Lee, S., Shinano, T., Onda, Y., Hayashi, S., 2019. Factors controlling dissolved ^{137}Cs concentrations in east Japanese Rivers. Sci. Total Environ. 697, 134093 https://doi.org/10.1016/j.scitotenv.2019.134093.

Tsuji, H., Nishikiori, T., Yasutaka, T., Watanabe, M., Ito, S., Hayashi, S., 2016. Behavior of dissolved radiocesium in river water in a forested watershed in Fukushima Prefecture. J. Geophys. Res. Biogeosciences. 121, 2588–2599. https://doi.org/10.1002/2016JG003428.

Tsuji, H., Yasutaka, T., Kawabe, Y., Onishi, T., Komai, T., 2014. Distribution of dissolved and particulate radiocesium concentrations along rivers and the relations between radiocesium concentration and deposition after the nuclear power plant accident in Fukushima. Water Res. 60, 15–27. https://doi.org/10.1016/j.watres.2014.04.024.

Tsuji, H., Nishikiori, T., Ito, S., Ozaki, H., Watanabe, M., Sakai, M., Ishii, Y., Hayashi, S., 2023. Influential factors of long-term and seasonal ^{137}Cs change in agricultural and forested rivers: temperature, water quality and an intense Typhoon event. Environ. Pol. 338, 122617 https://doi.org/10.1016/j.envpol.2023.122617.

Tsukada, H., Nihira, S., Watanabe, T., Takeda, S., 2017. The ^{137}Cs activity concentration of suspended and dissolved fractions in irrigation waters collected from the 80 km zone around TEPCO's Fukushima Daiichi Nuclear Power Station. J. Environ. Radioact. 178–179, 354–359. https://doi.org/10.1016/j.jenvrad.2017.08.002.

Ueda, S., Hasegawa, H., Kakiuchi, H., Akata, N., Ohtsuka, Y., Hisamatsu, S., 2013. Fluvial discharges of radiocaesium from watersheds contaminated by the Fukushima dai-ichi nuclear power plant accident, Japan. J. Environ. Radioact. 118, 96–104. https://doi.org/10.1016/j.jenvrad.2012.11.009.

Wauters, J., Elsen, A., Cremers, A., Konoplev, A.V., Bulgakov, A.A., Comans, R.N.J., 1996. Prediction of solid/liquid distribution coefficients of radiocesium in soils and sediments. Part one: a simplified procedure for the solid phase characterization. Appl. Geochem. 11, 589–594.

Wauters, J., Sweeck, L., Valcke, E., Elsen, A., Cremers, A., 1994. Availability of radiocaesium in soils: a new methodology. Sci. Total Environ. 157, 239–248. https://doi.org/10.1016/0048-9697(94)04287-W.

Yamasaki, S., Imoto, J., Furuki, G., Ochiai, A., Ohnuki, T., Sueki, K., Nanba, K., Ewing, R. C., Utsunomiya, S., 2016. Radioactive Cs in the estuary sediments near Fukushima Daiichi nuclear power plant. Sci. Total Environ. 551–552, 155–162. https://doi.org/10.1016/j.scitotenv.2016.01.155.

Yamashiki, Y., Onda, Y., Smith, H.G., Blake, W.H., Wakahara, T., Igarashi, Y., Matsuura, Y., Yoshimura, K., 2014. Initial flux of sediment-associated radiocesium to the ocean from the largest river impacted by Fukushia Daiichi Nucear Powe Plant. Sci. Rep. 4, 3714. https://doi.org/10.1038/srep03714.

Yoshimura, K., Onda, Y., Sakaguchi, A., Yamamoto, M., Matsuura, Y., 2015. An extensive study of the concentrations of particulate/dissolved radiocaesium derived from the Fukushima Dai-ichi Nuclear Power Plant accident in various river systems and their relationship with catchment inventory. J. Environ. Radioact. 139, 370–378. https://doi.org/10.1016/j.jenvrad.2014.08.021.

Yousef, Y.A., Kudo, A., Gloyna, E.F., 1970. Radioactivity Transport in Water-Summary Report. Report ORO-490, 20. United States Department of Energy.